Optical pump concepts for highly efficient quasi-three-level lasers

Klaus Albers · Ulrich Wittrock

Abstract Efficient quasi-three-level laser operation requires the generation of the highest possible pump rate from a given pump source. We derive the fundamental scaling laws for the pump rate and we extract optimization criteria for pump concepts from these laws. The analysis is then applied to the thin-disk laser. Based on the results, a novel pump concept for thin-disk lasers is proposed, which allows for several tens of pump beam passes and reduces the optical complexity of conventional pump concepts. Furthermore, the beam quality of the pump source is preserved almost completely, facilitating the highest possible pump rate.

K. Albers and U. Wittrock

Muenster University of Applied Sciences

Photonics Laboratory

Stegerwaldstrasse 39

48565 Burgsteinfurt, Germany

Tel.: +49-2551-962332

Fax: +49-2551-962705

E-mail: k.albers@fh-muenster.de

E-mail: wittrock@fh-muenster.de

1 Introduction

Optically pumped solid state lasers are essentially brightness converters. They transform the partially coherent radiation of lamps or diode lasers into highly coherent laser beams of somewhat lower optical power but much higher brightness. The great improvement in the brightness of high-power solid state lasers over the past two decades can mainly be attributed to improvements in the optical pump sources: switching from lamps to diode lasers in the nineties provided a great leap in pump source brightness, and the brightness of diode lasers has rapidly increased since then. These improvements facilitated laser concepts such as the cladding-pumped fiber laser and the thin-disk laser. Unlike the original lamp-pumped rod laser, these laser concepts can not convert completely incoherent radiation into a fully coherent single-mode beam. However, they are very efficient at converting partially coherent light into fully coherent or almost fully coherent light. The solid state laser as a brightness converter generally becomes more efficient if the brightness of the incoming radiation increases because less entropy and energy must be expelled to the environment. Therefore, it is wise to conserve and exploit the brightness of the pump source to the maximum possible extent.

In this paper we begin with some general thoughts about optimum pumping schemes for quasi-three-level lasers, and then we analyze the traditional pump concept for thin-disk lasers. Finally, we present a novel pump concept that better preserves and exploits the brightness of diode lasers. The novel pump concept is advantageous for many solid state laser media but particularly for quasi-three-level lasers and other laser media that have a high laser threshold, such as the up-coming blue-diode-pumped Praseodymium-doped lasers [1,2] or Ti:sapphire lasers [3].

The advantage of quasi-three-level lasers, as opposed to four-level-lasers, is the low quantum defect of the laser transition, enabling high efficiency and strongly reduced heat generation. However, quasi-three-level lasers can only be efficient when transparency at the lasing wavelength is achieved with as little pump power as possible. This requires the absorption of as much pump light as possible in as small a volume as possible. The most important design driver for the pump concept is therefore to concentrate the pump light in the smallest possible volume. Two laser geometries excel in this regard, namely the thin-disk laser [4,5] and the fiber laser [6,7]. Both concepts have been developed to take maximum advantage of the brightness of the pump laser diodes in order to maximize the pump light concentration.

In the following, we will analyze the physical and technical limits for the pump light concentration. Based on this analysis, we propose a novel pumping scheme for thin disk lasers. This novel pumping scheme has two advantages. First, it is using much simpler optics than the conventional pumping scheme for thin disk lasers. Second, it can achieve higher pump rates. This is especially important in quasi-three-level gain media that need even higher pump rates for achieving transparency than Yb:YAG. For such materials, a large fraction of the pump power has to be expended in order just to make the gain medium transparent.

2 Efficient pumping of quasi-three-level lasers

The pump power density required to make a quasi-three level medium transparent depends on the fractional thermal population density $\overline{n}_{1,thermal}$ of the lower laser level. $\overline{n}_{1,thermal} = \frac{n_{1,thermal}}{n}$ is the ratio of the density $n_{1,thermal}$ of ions that are thermally

excited into the lower laser level to the total active ion density n. Transparency is achieved if the fractional population density of the upper laser level, $\overline{n}_2 = \frac{n_2}{n}$, equals $\overline{n}_1$. At transparency, we have $\overline{n}_{2,trans} = \overline{n}_{1,thermal}$. With a good pump concept, $\overline{n}_{2,trans}$ is achieved with very little pump power. The excess pump power can then be used to operate the laser comparable to a four-level laser.

The process of populating the upper laser level is described by rate equations. These rate equations incorporate a pump rate W, which is the rate at which ions are excited into the upper laser level. The pump rate is opposed by loss processes such as spontaneous emission losses, amplified spontaneous emission, or up-conversion. The steady-state population density of the upper laser level is reached when the sum of all rates is zero. In order to reach $\overline{n}_{2,trans}$ with very little pump power, we have to maximize the pump rate W. The minimization of the loss rates is equally important but will not be considered within the scope of this analysis. A general equation for the pump rate W is given by

$$W = \sigma_{abs} \cdot n_0 \cdot \frac{P}{h\nu A} \tag{1}$$

σ_{abs} is the absorption cross-section, n_0 is the total population density of the ground-state multiplett, P is the pump power incident on the pumped area A, and $h\nu$ is the energy of the pump photons. The pump rate W states the number of pumping events per second and per volume that occur at a certain point in the gain medium. We do not consider the spectral overlap of the pump source and the active medium, the thermal occupation of the exact level in the ground-state we are pumping from, the transverse spatial distribution of the pump light, the temperature dependence of the absorption cross-section, or any other more advanced effect. Even if all these effects were

implemented, the pump rate is always increased by increasing the fraction $\frac{P}{A}$. Since the pump power P is usually given by the available pump source, we will concentrate on the minimization of the pumped area A. Assuming we have a stigmatic pump beam and a pump spot diameter D_{pump}, the pumped area is given by $A = \pi \frac{D_{pump}^2}{4}$. The pump spot diameter scales with the full divergence angle θ of the focused pump beam, the beam propagation factor M^2, and the pump wavelength λ by $D_{pump} = \frac{4M^2\lambda}{\pi\theta}$ [8]. At the waist of the pump beam, the pump rate becomes:

$$W = \sigma_{abs} \cdot n_0 \cdot \frac{\pi \, P \, \theta^2}{4 \, h\nu \, (M^2)^2 \, \lambda^2} \tag{2}$$

For a given medium and a given pump source, optimizing the pump geometry therefore requires that the pump-beam shaping optics preserves the pump power and the beam quality of the pump light. At the same time, the pump beam shaping optics should maximize the divergence angle θ of the focused pump beam in order to achieve the smallest possible waist in the gain medium.

Equation 2 is only valid for a disk-shaped section of the gain medium, located at the pump beam waist, whose thickness is small compared to the Rayleigh range of the pump beam. To build an efficient laser, a considerable fraction of the total pump power needs to be absorbed, requiring a certain absorption path length l. In almost all gain media, the required absorption path length is much longer than the Rayleigh range of the tightly focused pump beam. In this case, the spatially averaged pump rate is much lower than the pump rate at the beam waist given by equation 2. In end-pumped lasers, for instance, the beam waist is usually quite large, in order to avoid a strongly divergent pump beam within the gain medium. However, the pump beam diameter at the beam waist can in principle be maintained along the absorption
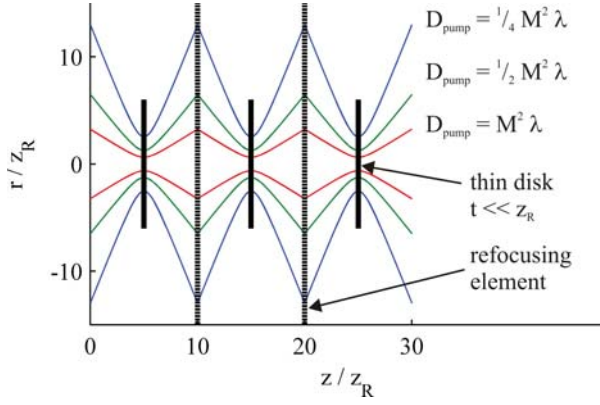
Fig. 1 Caustics of three pump beams successively focused onto thin disks with thickness t at different pump spot diameters D_{pump}.

path. One way to maintain the pump beam diameter is total internal reflection in a fiber. Another option would be successive re-imaging of the pump spot onto thin disks with a thickness t well below the Rayleigh range $z_R = \frac{\pi D_{pump}^2}{4\,M^2\,\lambda}$. The number of disks would need to be chosen such that the accumulated thickness of all the disks equals the length l, which is required for sufficient absorption. For illustrative purposes, this optical arrangement is shown in Figure 1. Between the thin disks, an optical element is used to refocus the pump spot onto the next thin disk. The graph shows the caustics of three pump beams with different pump spot diameters. The radial coordinate r and the propagation coordinate z are normalized to the Rayleigh range z_R to eliminate the caustic's dependence on a specific beam propagation factor. Because $z_R \sim D_{pump}^2$, small pump spot diameters appear large in this graph. Both axes of the graph are plotted on the same scale, so the well-known fact that the divergence angle of the pump light approaches π for pump spot diameters less than $D_{pump} = M^2\lambda$ can be observed. We do not consider that the paraxial approximation will no longer hold for very tight focusing. In this ideal pumping configuration, the minimum pump beam waist can be
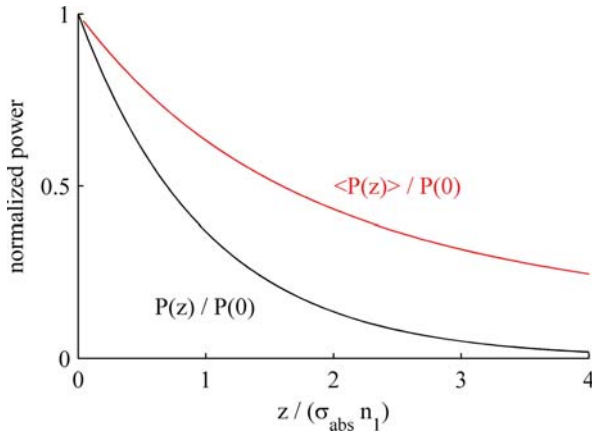
Fig. 2 Local pump power $P(z)$ and spatially averaged pump power $\langle P(z) \rangle$ for different propagation distances z.

maintained throughout the whole pumped volume. Therefore, two dimensions of the pumped volume are minimized without any further options for improvement. The third dimension of the pumped volume depends on the properties of the active medium and the required absorption efficiency, which will be analyzed in the following.

The local pump power $P(z)$ passing through the medium varies along the propagation distance z as illustrated by the curve $P(z)/P(0)$ in Figure 2 for a single pass of the pump light. The spatially averaged pump power $\langle P(z) \rangle$ passing through a pumped volume of length z is given by

$$\langle P(z) \rangle = \frac{1}{z} \int_0^z P(z)\, \mathrm{d}z = \frac{P(0)}{\sigma_{abs}\, n_0\, z} \left(1 - \mathrm{e}^{-\sigma_{abs}\, n_0\, z} \right) \tag{3}$$

It is decreasing with increasing length of the pumped volume. Put the other way round, a demand for better pump light absorption leads to a decrease of the spatially averaged pump power passing through the medium. The absorbed pump power P_{abs} can be written as $P_{abs} = \eta_{abs}\, P$. We define the absorption efficiency η_{abs} as the fraction of the pump light that is absorbed by the pumped medium, i. e., $\eta_{abs} = 1 - \mathrm{e}^{-2\sigma_{abs}\, n_0\, l}$.

We added a factor of 2 to the exponent to account for double-pass pumping. l is the accumulated thickness of all disks with thickness t according to figure 1. Since the optical configuration of figure 1 allows us to maintain the beam waist diameter throughout the whole pumped volume, the equation for the pumped volume V is given by

$$V = \pi \frac{D_{pump}^2}{4} \, l = \frac{4 \left(M^2\right)^2 \lambda^2}{\pi \theta^2} \, l \tag{4}$$

The spatially averaged pump rate $\langle W \rangle$ within the pumped volume V is then given by

$$\langle W \rangle = \sigma_{abs} \cdot n_0 \cdot \frac{\langle P(l) \rangle}{h\nu \, A} = P \left(1 - \mathrm{e}^{-2\sigma_{abs} \, n_0 \, l}\right) \frac{\pi \, \theta^2}{4 \, h\nu \, \left(M^2\right)^2 \lambda^2 \, l} \tag{5}$$

Equation 5 can be rewritten by expressing $1 - \mathrm{e}^{-2\sigma_{abs} \, n_0 \, l}$ and l in terms of η_{abs}:

$$\langle W \rangle = -\frac{\eta_{abs} \, \theta^2}{\ln\left(1 - \eta_{abs}\right)} \cdot \sigma_{abs} \, n_0 \cdot \frac{\pi \, P}{2 \, h\nu \, \left(M^2\right)^2 \lambda^2} \tag{6}$$

Equation 6 has been separated into three characteristic fractions. The first fraction depends only on the absorption efficiency η_{abs} and the solid angle of the focused pump beam (approximately proportional to θ^2), which are both determined by the pump geometry. The second fraction depends only on the properties of the active medium. The third fraction represents the properties of the pump source. As can be seen, the average pump rate is not just proportional to η_{abs} because both the length of the pumped volume and the spatial average of the pump power depend on η_{abs}, which is illustrated in Figure 2. In the limit of $\eta_{abs} \to 0$, we obtain $-\frac{\eta_{abs}}{\ln(1-\eta_{abs})} = 1$ and equation 6 becomes equal to equation 2, apart from the factor of 2 for double-pass pumping. An efficient laser requires the absorption of most of the pump light. According to the Lambert-Beer law, the absorption efficiency η_{abs} can only approach the ideal value of 1 in the limit of $l \to \infty$. A realistic value for η_{abs} is 95 %, which requires a laser medium of length $l = \frac{1}{2} \frac{3}{\sigma_{abs} n_0}$ in the case of double-pass pumping. With such efficient

pump light absorption we have a reduction of the average pump rate $\langle W \rangle$ by a factor of $-\frac{\eta_{abs}}{\ln(1-\eta_{abs})} \approx \frac{1}{3}$ compared to the case of $\eta_{abs} \rightarrow 0$. For a practical laser, a compromise between a high value of $\langle W \rangle$ and a high value of η_{abs} must be made. The optimum compromise is determined not only by the thermal population of the lower laser level of the particular gain medium but also by other parameters such as the available pump power.

According to the analysis above, the maximization of the pump light concentration requires first of all to use the pump source with the highest available brightness, which is proportional to $\frac{P}{(M^2)^2}$. The brightness of the pump source needs to be conserved by the pump beam shaping optics, which may be a complicated task, especially, if very astigmatic diode laser bars are involved. In order to achieve the highest possible spatially averaged pump rate, the pump geometry should focus the pump light to the smallest possible diffraction-limited pump beam diameter and this diameter needs to be maintained throughout the pumped volume. This task requires focussing at the largest possible solid angle and a potentially complicated optical system to maintain the beam diameter. The absorption cross-section of the medium should be as high as possible within the spectral bandwidth of the pump source, in order to minimize the length of the pumped volume. Within the scope of the analysis presented here, an increase of the doping concentration n is not beneficial, since we are interested in the fractional population density $\frac{\overline{n}_{2,trans}}{n}$. When considering the temperature of the laser medium, an increase in doping concentration may improve the laser, as it is true for thin disk lasers.

3 Optical pump concepts

One pump concept suitable for achieving a high spatially averaged pump rate $\langle W \rangle$ of the upper laser level and efficient pump absorption is the fiber laser. A pump beam can be focused into a fiber with a diameter on the order of $M^2\lambda$, if the solid angle of the pump focusing optics approaches 2π, corresponding to a numerical aperture of 1. The pumped volume will then be on the order of magnitude of $\left(M^2\lambda\right)^2 l$. A double-clad fiber needs to be analyzed in a bit more detail. It needs to be longer than the absorption length of $l = \frac{1}{2}\frac{3}{\sigma_{abs}n}$, because the diameter of the pump cladding is larger than the core diameter. On a single "zig" of the pump light across the fiber, the pump light is only absorbed within the core. The required number of "zigs" through the fiber core is equal to the required absorption path length divided by the average path length through the core per "zig". The required length of the fiber is then given by the number of "zigs" multiplied by the average length of the fiber per "zig". This can result in quite long fibers. Nevertheless, the pumped fiber core volume is still of the order of magnitude of $\left(M^2\lambda\right)^2 l$, just as for a single-clad fiber. The reason is that the core diameter of a double-clad fiber is much smaller than $\left(M^2\lambda\right)$, which is the diameter of pump cladding. This is compensated by the larger length of the double-clad fiber compared to a single-clad fiber. To create a stigmatic beam that can be matched to a fiber, complex pump beam shaping for the astigmatic light emitted from diode bars is necessary. This leads to some loss of power and an increased beam propagation factor. Nevertheless, the fiber concept is currently the pump concept able to create the highest spatially averaged pump rate. The pump light is guided by total internal reflection and can thus exploit a very large solid angle by means of an extraordinary simple optical

half sphere above the thin disk
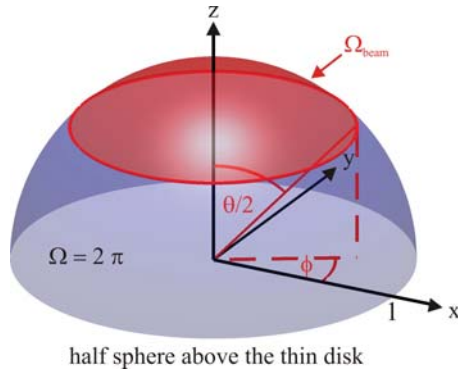
Fig. 3 Illustration of the solid angle Ω_{beam} occupied by a rotationally symmetric beam with a full divergence angle θ.

system.

We now return to the multi-disk pump concept of figure 1. If we change the transmissive refocusing systems into reflective ones and use only one disk pumped from many directions, then we arrive at the well-known thin-disk laser. This approach, of course, is much more practical. However, it comes at the expense that one can not use a large numerical aperture for focusing the beam. The reason for this inability is that the solid angle of 2π above the disk must be used for arranging the different beam paths. The lower numerical aperture leads to a larger pump spot compared to the multi-disk laser. The disadvantage of the larger pump spot is cancelled out by the possibility of reducing the disk's thickness proportional to the number of pump beams, resulting again in a very small pumped volume. Furthermore, the thin disk facilitates cooling which reduces $\overline{n}_{1,thermal}$. In the following, we will derive the scaling laws for the spatially averaged pump rate $\langle W \rangle$ in a thin-disk laser.

The solid angle Ω_{beam} of one single pump beam with a full divergence angle θ can be calculated according to the drawing in Figure 3 by the following equation:

$$\Omega_{beam} = \int_0^{2\pi} \int_0^{\frac{\theta}{2}} \sin\theta \, d\theta \, d\phi = 2\pi \left(1 - \cos\frac{\theta}{2} \right) \tag{7}$$

Using the beam parameter product, we can replace θ according to equation 8:

$$\theta = \frac{4M^2\lambda}{\pi D_{pump}} \tag{8}$$

The equation for the solid angle of one pump beam is then given by

$$\Omega_{beam} = 2\pi \left[1 - \cos\left(\frac{2M^2\lambda}{\pi D_{pump}} \right) \right] \tag{9}$$

If we arrange several pump beams in a cone with full divergence angle θ_{cone}, then the maximum number N_{max} of separate beams that theoretically fit into the cone is given by

$$N_{max} = \frac{\Omega_{cone}}{\Omega_{beam}} = \frac{1 - \cos\left(\frac{\theta_{cone}}{2} \right)}{1 - \cos\left(\frac{2M^2\lambda}{\pi D_{pump}} \right)} \tag{10}$$

Since we restricted the discussion to circular pump beams, the cone can not be covered completely by pump beams, which is easily understood by visualizing the coverage of only three pump beams ($N = 3$). We neglect such fill-factor limitations and calculate only an upper limit for N_{max}. Each of the N_{max} pump beams double-passes the thin disk with thickness t. The spatially averaged pump power $\langle P \rangle$ inside the pumped volume is then given by

$$\langle P \rangle = \frac{P}{\sigma_{abs}\, n_0\, t} \left(1 - e^{-2N_{max}\sigma_{abs}\, n_0\, t} \right) \tag{11}$$

Similar to equation 5, the equation for the spatially averaged pump rate $\langle W \rangle$ is then given by

$$\langle W \rangle = \sigma_{abs}\, n_0 \cdot \frac{4\,\langle P \rangle}{h\nu\, \pi\, D_{pump}^2} = \frac{4\, P \left(1 - e^{-2N_{max}\sigma_{abs}\, n_0\, t} \right)}{h\nu\, \pi\, D_{pump}^2\, t} \tag{12}$$
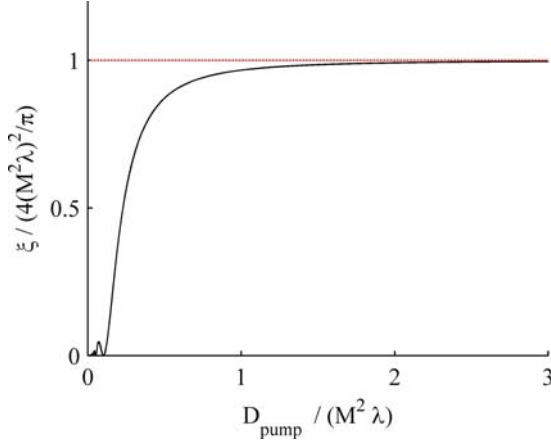
Fig. 4 Denominator $\xi = 2\pi D_{pump}^2 \cdot \left[1 - \cos\left(\frac{2M^2\lambda}{\pi D_{pump}} \right) \right]$ of equation 14 versus D_{pump}.

For the thin disk laser, the absorption efficiency is given by $\eta_{abs} = \left(1 - e^{-2N_{max}\sigma_{abs}\,n_0\,t} \right)$. Expressing the terms $\left(1 - e^{-2N_{max}\sigma_{abs}\,n_0\,t} \right)$ and t in terms of η_{abs} results in equation 13:

$$\langle W \rangle = -\frac{16\eta_{abs}}{\ln\left(1 - \eta_{abs} \right)} \cdot \sigma_{abs}\, n_0 \cdot \frac{P}{h\nu} \cdot \frac{N_{max}}{2\pi D_{pump}^2} \tag{13}$$

Substituting N_{max} in equation 13 by equation 10 leads to:

$$\langle W \rangle = -\frac{16\eta_{abs}}{\ln\left(1 - \eta_{abs} \right)} \cdot \sigma_{abs}\, n_0 \cdot \frac{P}{h\nu} \cdot \frac{1 - \cos\left(\frac{\theta_{cone}}{2} \right)}{2\pi D_{pump}^2 \left[1 - \cos\left(\frac{2M^2\lambda}{\pi D_{pump}} \right) \right]} \tag{14}$$

Figure 4 illustrates the behavior of the denominator ξ of the last term in equation 14:

$$\xi = 2\pi D_{pump}^2 \cdot \left(1 - \cos\left(\frac{2M^2\lambda}{\pi D_{pump}} \right) \right) \tag{15}$$

For physically meaningful pump spot diameters $D_{pump} \geq M^2\lambda$, the denominator rapidly settles at its asymptotic value for $D_{pump} \to \infty$:

$$\lim_{D_{pump} \to \infty} \xi = \frac{4\left(M^2\lambda \right)^2}{\pi} \tag{16}$$

Implementing this result into equation 14 results in

$$\langle W \rangle = -\frac{\eta_{abs}}{\ln\left(1 - \eta_{abs} \right)} \cdot \sigma_{abs}\, n_0 \cdot \frac{4\pi P \cdot \left(1 - \cos\left(\frac{\theta_{cone}}{2} \right) \right)}{h\nu \left(M^2 \right)^2 \lambda^2} \tag{17}$$

The Taylor expansion of $\left[1 - \cos\left(\frac{\theta_{cone}}{2}\right)\right]$ up to the quadratic term is equal to $\left[\frac{1}{8} \cdot \theta_{cone}^2\right]$.

Substituting this into equation 17 we obtain the final equation for the average pump

rate in a thin disk laser:

$$\langle W \rangle = -\frac{\eta_{abs}\,\theta_{cone}^2}{\ln\left(1 - \eta_{abs}\right)} \cdot \sigma_{abs}\,n_0 \cdot \frac{\pi P}{2\,h\nu\,(M^2)^2\,\lambda^2} \tag{18}$$

Thus, the spatially averaged pump rate for multipass pumping is identical to the pump

rate given earlier by equation 6 for double-pass pumping. It is interesting to note that

the exploitation of the brightness of the pump source just requires to use the largest

possible solid angle to direct the pump light into the medium. Whether only a single

beam or many optically recycled beams are used has no influence on the result. The

pump concentration is simply proportional to the absolute solid angle. The pumped

volume of the thin disk laser is given by

$$V = \pi \cdot \frac{D_{pump}^2}{4} \cdot t \tag{19}$$

The thickness t of the disk has to equal the required absorption length l divided by

the number of pump beams N_{max}:

$$t = \frac{l}{N_{max}} \tag{20}$$

As can be shown, the minimum pump spot area that can be achieved with N_{max} beams

is N_{max} times larger than the minimum pump spot area that can be achieved by a

single beam covering the same solid angle. Therefore, the smallest possible pumped

volume in the thin disk laser is of the order of $V_{min} = \pi\frac{\left(M^2\lambda\right)^2}{4}l$, which is equal to the

smallest possible pumped volume of the multi disk pumping scheme from chapter 2 of

this paper.

The conventional thin disk setup [9,10] is shown in Figure 5. A pump beam is
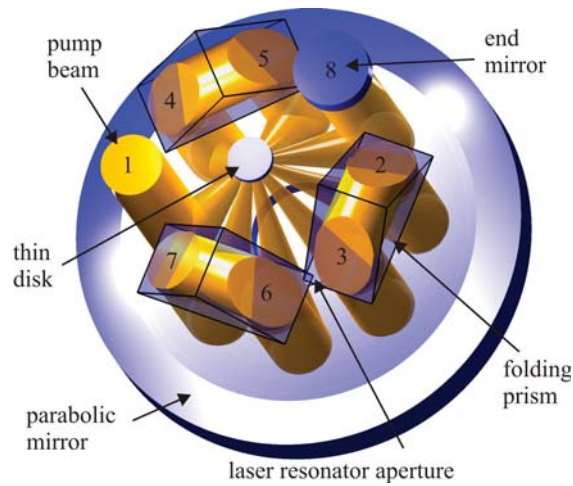
Fig. 5 Conventional thin disk pumping scheme.

guided four times back and forth through a thin disk and, afterwards, is reflected by an end mirror to make four additional double passes through the disk. The resulting absorption pathlength is 16 times the disk thickness t. In this configuration, however, much of the solid angle above the thin disk remains unused because the beams are arranged on the parabolic mirror in an annulus and neither the area inside nor outside of the annulus is used. Consequently, the brightness of the pump source is not fully exploited, and the pumped volume is larger than its theoretical minimum. Figure 6 shows a theoretical solution for better exploitation of the pump brightness. The pump beams are arranged in multiple rings to fill up the solid angle. This, of course, would require a very complex optical system. Therefore, the pumping scheme of thin disk lasers is usually constrained to only one ring of circular pump beams.

In the following, an upper limit for the total solid angle Ω covered by all of the combined pump beams is calculated for a given number N of stigmatic pump beams arranged in a single ring. The total solid angle Ω is maximized if the solid angle Ω_{beam}
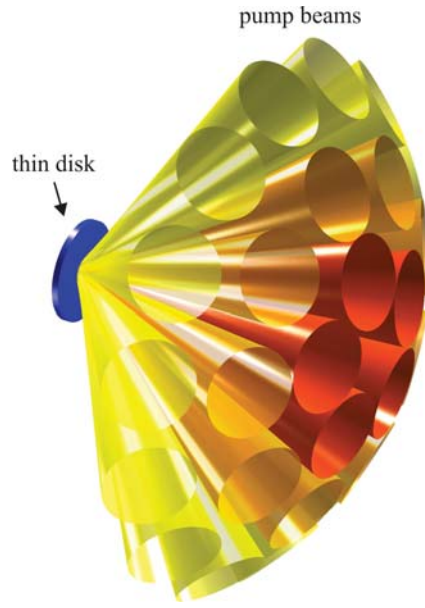
Fig. 6 Thin-disk pumping scheme with multiple rings of stigmatic pump beams.

of each beam is as large as possible. This requires the beams to be arranged at the maximum possible angle between their optical axis and the axis of the disk. We do not consider the deformation of the pump spot at such extreme focusing angles. The following calculation is based on the drawings shown in Figure 7. If θ denotes the full divergence angle of each pump beam, then the maximum angle between the optical axis of the beam and the axis of the thin disk (z-axis in figure 7) equals $\pi/2 - \theta/2$. As shown in figure 7, all of the optical beam axes intersect the half sphere of radius R on a circle of radius $r = R \cdot \cos \frac{\theta}{2}$. The maximum number of beams N in this arrangement is then given by the circumference of the circle divided by the arc length $R\theta$ covered by each beam along the circle:

$$N = \frac{2\pi R \cos \frac{\theta}{2}}{R\theta} = \frac{2\pi \cos \frac{\theta}{2}}{\theta} \tag{21}$$
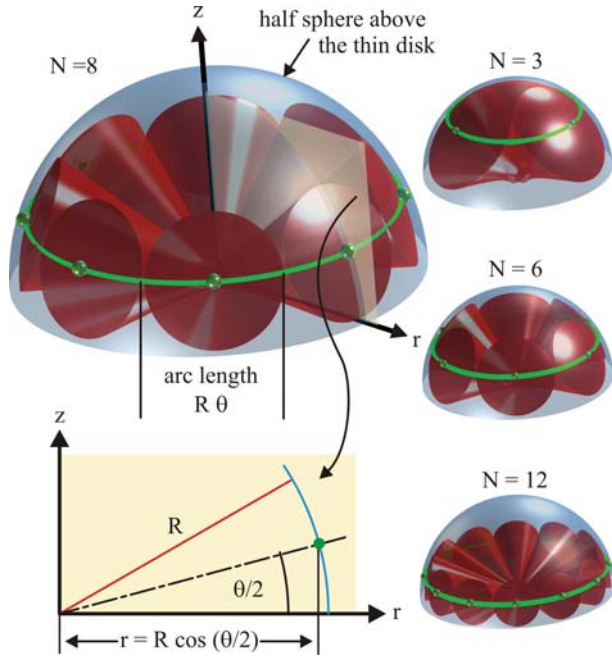
Fig. 7 Illustration of the total solid angle Ω above the thin disk covered by a single ring of N pump beams.

The accumulated solid angle Ω of all the pump beams is

$$\Omega = N \cdot \Omega_{beam} = N \cdot 2\pi \left(1 - \cos \frac{\theta}{2} \right) \tag{22}$$

Figure 8 shows the attainable relative coverage $\Omega_{frac} = \frac{\Omega}{2\pi}$ of the half sphere above the thin disk for a single ring of N pump beams. The value of Ω has been obtained by numerically solving equation 21 for a given N and then using equation 22 with the calculated value for θ. The maximum coverage is 100 % for a single beam, which completely uses up the solid angle above the disk. The second-best coverage is an arrangement of three beams with a full divergence angle of $\theta = 80°$. This arrangement results in 80 % coverage of the solid angle above the disk. For a conventional thin-disk laser with eight pump beams, the theoretical coverage for close-packed beams can be as high as 50 %. In practice, only a somewhat lower fractional use of the solid angle is
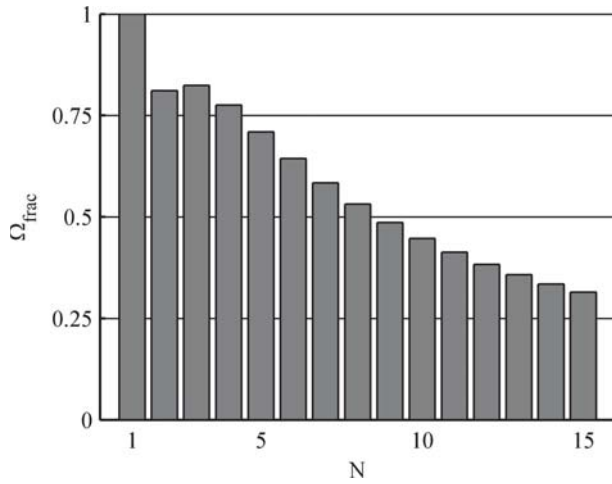
Fig. 8 Maximum pump light covering Ω_{frac} of the half sphere above a thin disk pumped by a single ring of N pump beams.

possible.

To conclude, the highest efficiency of a quasi-three-level thin-disk laser can be expected when the disk is pumped from almost the complete solid angle of 2π because this results in the highest spatially averaged pump rate. The brightness of the pump source should be conserved by the pumping scheme, which is a great challenge because the highly astigmatic beam of the diode laser has to be shaped into a stigmatic beam. The temperature in the thin disk is proportional to the square of the disk's thickness, as long as the heating power and the pump spot diameter are kept constant. This means that the disk should be made as thin as possible, resulting in a lower value for $\overline{n}_{1,thermal}$. Thinner disks require more pump beam passes to achieve the required absorption. An increase according to figure 7 would lead to a lower fractional coverage of the solid angle above the disk and thus to a lower pump rate. Increasing the number of pump beam passes according to Figure 6 would lead to very complex optical ar-

rangements. The absorption could alternatively be increased by increasing the doping concentration of the active laser ion. Unfortunately, the doping concentration of the laser ions is often limited by a variety of detrimental effects, such as concentration quenching or up-conversion.

In the following, we present a novel thin-disk pumping scheme that allows for simple scaling of the number of pump beam passes. Furthermore, the brightness of the pump diode laser is conserved almost completely because the pump beam is not made stigmatic. Finally, the solid angle above the laser disk can be used almost completely, which means that a very high pump light concentration can be achieved.

4 Novel pumping scheme

The proposed pumping scheme is intended to maximize the spatially averaged pump rate $\langle W \rangle$ for a thin disk pumped by a single laser diode bar, but the concept can be adapted for diode-stacks as well. The motivation for using diode bars instead of fiber-coupled pump sources is the conservation of the diode bar's brightness. Due to the asymmetric beam parameters of diode bars, mode-matching between diode bars and circular fibers is a complicated task and results in brightness losses due to both coupling losses and beam quality degradation. The beam quality of a typical fiber-coupled diode laser is reduced by at least a factor of two compared to the naked bar and the optical power loss is approximately 20 %. If fast-axis collimated bars without fiber coupling are used instead, then both the beam quality and the output power of the naked bar can be preserved. The proposed pumping scheme makes use of the asymmetry of the

pump beams

thin disk

diode laser's
fast axis

diode
laser's
slow
axis
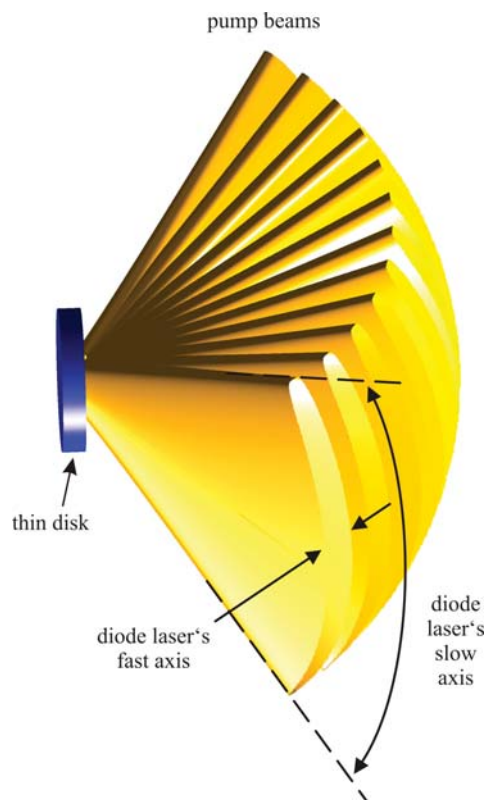
Fig. 9 Multiple focused diode laser beams folded along their fast-axis direction.

diode beam instead of trying to convert it into a circular beam.

According to the beam parameter product, focussing an astigmatic diode laser bar's beam into a symmetric pump spot with a spot diameter D_{pump} requires that the ratio of the focusing angles of the slow-axis and fast-axis is M_{sa}^2/M_{fa}^2. For typical pump spot sizes in the mm-range, the necessary slow-axis divergence angle approaches $90°$, while the fast-axis divergence angle is on the order of 1 mrad. The one-dimensional extent of the halfsphere above the thin disk is equal to $\frac{1}{2}$ rad. In the fast-axis direction, we can therefore arrange several hundred beams inside the halfsphere. Figure 9 illustrates such a pumping geometry with 12 exemplary pump beams. The propagation distance

of the beams shown is well below the Rayleigh range of the fast-axis, such that the maximum number of beams in this example is limited by the fast-axis near-field width rather than by the fast-axis far-field angle. This can be understood by visualizing the beams close to the disk, where they overlap and can not be separated by an optical system. At a large enough distance from the thin disk, the beams separate spatially if their far-field divergence angle is smaller than the angle between neighbouring beam axes. The ultimate limit for the number of beams is their separability in the farfield of the fast-axis. In Figure 9, the divergence angle of the slow axis is chosen not as large as possible. With a good optical system such as a parabolic mirror, the divergence angle can be increased without introducing aberrations up to a theoretical limit of π. Therefore, almost the complete solid angle above the thin disk could be covered by using more beams and larger focusing angles. This is different from the conventional thin disk pumping scheme with a single ring of circular pump beams, which allows only a partial coverage of the solid angle above the disk, as shown in figure 8.

To angle-multiplex a fast-axis collimated pump beam according to the pumping scheme shown in Figure 9, the optical setup shown in Figure 10 can be used. The parabolic mirror re-images the pump spot onto itself, while the necessary beam displacement is achieved by two simple planar folding mirrors. The number of passes and the displacement of the beams can simply be adjusted by translating the folding mirrors. The focal length f of the parabolic mirror should be greater than or equal to the Rayleigh range of the fast-axis. Only in this case the number of beams can reach the theoretical maximum because the spatial separation of the beams takes place in the farfield of the fast-axis. For a symmetrical pump spot, the minimum pump spot diameter is on the order of $D_{pump} = M_{sa}^2 \lambda$. From the last two statements, we obtain
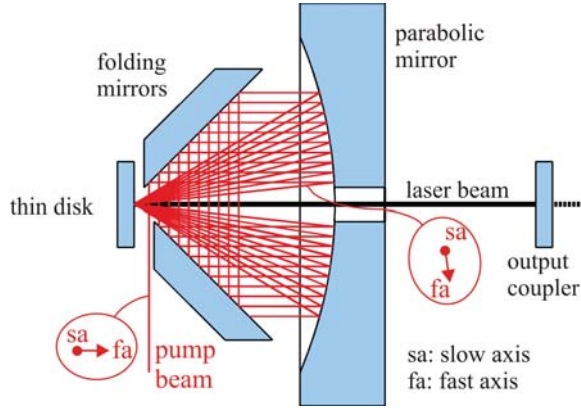
Fig. 10 Optical pumping scheme for one-dimensional folding of fast-axis collimated diode beams along their fast-axis direction.

an expression for the minimum focal length of the parabolic mirror:

$$f \geq z_R^{fa} = \frac{\pi D_{pump}^2}{4 M_{fa}^2 \lambda} \approx \frac{\left(M_{sa}^2\right)^2}{M_{fa}^2} \lambda \tag{23}$$

For the typical high-power diode laser bars mentioned above, the required focal length would be in the range of one meter, resulting in an extraordinarily large parabolic mirror. One possible solution for using a mirror with a shorter focal length is to generate an asymmetric pump spot by tighter focusing of the fast-axis. Another solution is to use slow-axis collimated diode bars, which provide a slow-axis beam propagation factor improvement by a factor of 2. However, even if the number of passes is limited by the fast-axis near-field width, several tens of pump beams fit into the half sphere above the disk. It is not shown in figure 10, but the pump beam can be reflected after its last pass to retrace its path and double the number of passes through the disk.

A photograph of a first experimental realization of the novel pumping scheme is shown in Figure 11. For illustrative purposes, the thin disk has been replaced by a highly reflective mirror. A fast-axis collimated beam from a 40-W diode bar is directed
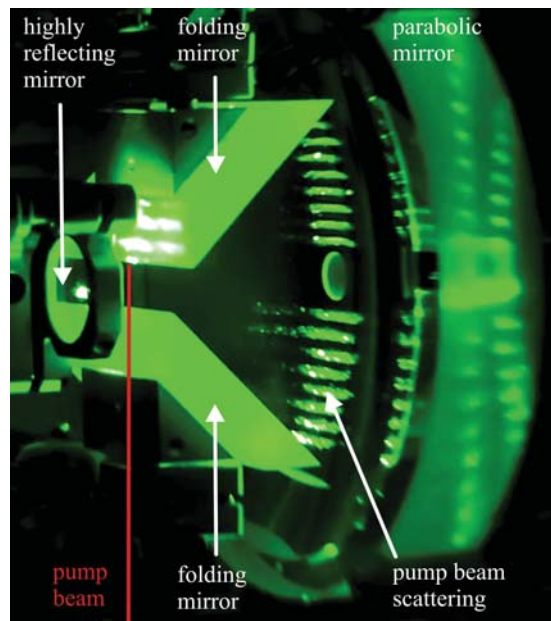
Fig. 11 Experimental multipass setup. The thin disk has been replaced by a highly reflecting mirror, and the invisible diode-laser input beam has been marked by the red line. The scattering of the 16 elongated diode laser footprints on the parabolic mirror is clearly visible.

from the bottom side towards the upper folding mirror directly in front of the highly reflective mirror. The beam is then angle-multiplexed according to the principle shown in Figure 10. With this setup, an absorption path length of up to 64 times the disk thickness has been realized. This means that an absorption path of 1 mm can be achieved with a disk that is only 16 μm thick. The slow-axis of the diode laser bar has not been magnified before entering the optical system. Therefore the coverage of the solid angle is rather low. However, the angle-multiplexing of the pump beam can clearly be realized with the proposed optical system. The measured pump spot on the highly reflecting mirror was stripe-like with an aspect ratio of 1:7, which is also due to the insufficient magnification of the slow axis. In the fast-axis direction, not all of the beams hit exactly the same location on the mirror which leads to a broadening of the
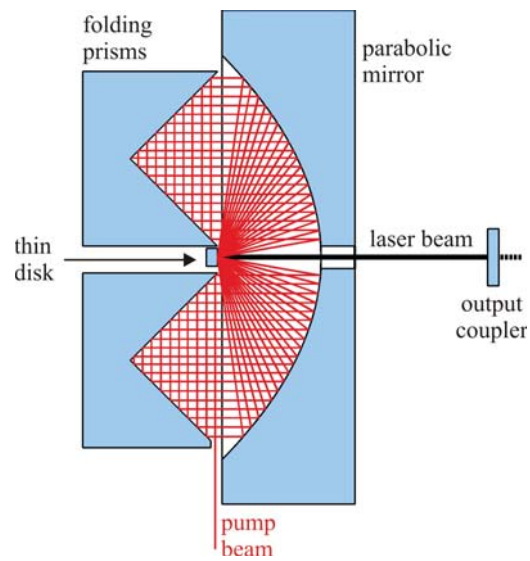
Fig. 12 Optical pumping scheme for one-dimensional folding of diode laser beams with maximum coverage of the solid angle.

pump spot and to the mentioned aspect ratio of 1:7. The aspect ratio would be even more extreme without this re-imaging error.

It is important to mention that the pumping scheme shown in Figure 10 does not allow coverage of the complete solid angle above the thin disk. Although the folding principle is beneficial due to its simplicity, the two plane folding mirrors limit the solid angle for the pump light because they form a $90°$ angle. With the slight modification shown in Figure 12, it is possible to completely fill the solid angle and, therefore, to exploit the brightness of the pump source to the maximum possible extent.

5 Conclusion

We have investigated the scaling laws for creating high pump rates in thin disk lasers. The ideal pump concept makes use of the complete solid angle outside of the pumped volume and conserves the brightness of the pump source to the maximum possible

extent. The required absorption efficiency needs to be chosen with respect to the parameters of the laser to be built, e.-g., the thermal occupation of the lower laser level of the active medium and the resonator roundtrip losses. We analyzed the conventional pump concept for thin-disk lasers which relies on a stigmatic beam. With this pumping geometry, it is both difficult to preserve the brightness of the pump source and to cover a large fraction of the solid angle above the thin disk. Based on these results, we proposed a novel thin-disk pumping geometry that preserves the beam quality of commonly used laser diode bars with asymmetric beam properties. The concept theoretically allows for the complete coverage of the solid angle above the thin disk and is optically very simple. There are two reasons for the higher pump rates that can be achieved with our novel pump concept:

– There are no losses in power and beam quality by transforming the diode bar's astigmatic beam into a stigmatic, fiber-coupled beam

– The astigmatic, rectangular beam of a fast-axis collimated diode bar is much better suited for multi-pass folding than a stigmatic beam. A large solid angle can be covered without any large voids.

With a first prototype, we achieved 32 double passes of the pump beam through a thin disk. Future work may concentrate on increasing the pump power density by spectrally combining multiple diode bars, which are wavelength stabilized and spectrally narrowed by volume bragg gratings. In addition, the pump power can simply be doubled by polarization-multiplexing of diode bars.

Even when only a limited number of pump-light passes is required, the novel pump concept is very attractive since it relieves the laser designer from pump beam sym-

metrization. The parabolic mirror could be replaced by a spherical mirror, if the solid angle covered by the pump beams is not too large. For low-power lasers, it may even be possible to implement the pumping scheme in a monolithic device made of transparent plastic.

References

1. A. Richter, E. Heumann, E. Osiac, G. Huber, W. Seelert, A. Diening, Opt. Lett. **29**(22), 2638 (2004). DOI 10.1364/OL.29.002638. URL http://ol.osa.org/abstract.cfm?URI=ol-29-22-2638

2. N. Hansen, A. Bellancourt, U. Weichmann, G. Huber, Applied optics **49**(20), 3864 (2010)

3. P. Roth, A. Maclean, D. Burns, A. Kemp, in *Conference on Lasers and Electro-Optics* (Optical Society of America, 2010)

4. A. Giesen, H. Huegel, A. Voss, K. Wittig, U. Brauch, H. Opower, Appl. Phys. B. **58**, 365 (1994)

5. A. Giesen, J. Speiser, IEEE Selected Topics in Quantum Electronics **13**(3), 598 (2007). DOI 10.1109/JSTQE.2007.897180

6. E. Snitzer, J. Appl. Phys. **32**, 36 (1961)

7. M.J.F. Digonnet (ed.), *Rare-Earth-Doped Fiber Lasers and Amplifiers* (CRC Press, 2nd edn., 2001)

8. A.E. Siegman, in *Tutorial presented at Optical Society of America Annual Meeting, Long Beach, California, October 1997*

9. S. Erhard, A. Giesen, M. Karszewski, T. Rupp, C. Stewen, in *OSA Trends in Optics and Photonics, Advanced Solid State Lasers*, vol. 26, ed. by M.M. Fejer, H. Injeyan, U. Keller (1999), vol. 26, pp. 38–44

10. S. Erhard, M. Karszewski, C. Stewen, A. Giesen, in *Advanced Solid State Lasers*, *OSA Trends in Optics and Photonics (TOPS)*, vol. TOPS 34, ed. by H. Injeyan, U. Keller, C. Marshall (OSA, Davos, Switzerland, 2000), *OSA Trends in Optics and Photonics (TOPS)*, vol. TOPS 34, pp. 78–84